J. Condensed Matter Nucl. Sci. 6 (2012) 77–89

Research Article

The Open Gate Phenomenon: A New Energy Technology

Susan L. Taft

Flowing Water Consulting, P.O. Box 709, Geneva, OH 44041 USA

Jan Marwan *

Dr Marwan Chemie, Rudower Chaussee 29, 12489 Berlin, Germany

Abstract

The Open Gate Phenomenon is a unique solid-state mechanism that results in a significant and sustained electron transfer from an n-type semiconductor to Schottky metal particles that are *grown from* the semiconductor substrate itself. This results in a unique interface that acts as a one-way (rectifying) open gate. First identified in reduced polycrystalline titanium dioxide (an n-type semiconductor) to Group VIII metal particles, the interface significantly affects the Schottky barrier height resulting in electron flow into the metal particles from the reduced titanim dioxide (TiO_2) based on their respective work functions. The result is a negative charge on the metal particles which is of sufficient magnitude and duration to provide cathodic protection of the metal particles from surface oxidation. In essence, the metal particles behave as a negatively charged electrode without an externally supplied power source.

Keywords: Microspheres, Pechini process, Polycrystalline, Submonolayer, X-ray photoelectron spectroscopy

1. Introduction

The data supporting the hypothesis of the Open Gate Phenomenon was collected thirty years ago where extremely unusual negative binding energy shifts below zero valence energies were observed for rhodium ($Rh3d_{5/2}$) on reduced titanium dioxide (TiO_2) using X-ray photoelectron spectroscopy (XPS). The discovery of the unusual negative binding energy shifts was the result of the initial failure to make a rhodium-doped TiO_2 material ($Ti_{0.99}\ Rh_{0.01}O_2$) to reduce the band gap for a TiO_2-based photoelectrochemical material using the Pechini process [1] to substitute Rh into the TiO_2 lattice. After formation of the resin intermediate from the Pechini process, the materials were subjected to high temperature oxidation and reduction, in excess of 1400°C. X-ray photoelectron spectroscopy (XPS) analysis was chosen to help verify Rh substitution by identifying its oxidation state. The binding energies for $Rh3d_{5/2}$ for materials prepared at three different temperatures (1400°C, 1600°C and 1650°C) were consistently far below below the reference of

*E-mail: info@marwan-chemie.fta-berlin.de

307.2 eV for Rh^0 [2] (301.2, 302.2, and 202.6 eV, respectively). This corresponds to negative binding energy shifts of 6.0, 5.0, and 4.6 eV below the reference for Rh^0, an extremely unusual occurrence. The binding energies for Ti2$p_{3/2}$ did not exhibit the same negative binding energy shifts. Subsequent scanning electron microscopy (SEM) examination using energy dispersive X-ray (EDX) analysis found that rhodium was observed in discrete particles on the surface of the crystalline TiO_2 material, *grown from* the TiO_2 substrate. The particles were both regularly and irregularly shaped microspheres from approximately 1–10 μm in size.

A subsequent literature search at the time (1981–1982) found three instances where negative binding energy shifts of metals were observed: (1) surface atom core-level shifts (SCLS), both positive and negative, relative to bulk [3], (2) metal alloys [4], and (3) submonolayer thin film coverage and small clusters [5–7]. In the case of SCLS, Johansson and Martensson [4] attributed the shifts to the difference in potential experienced by surface atoms relative to bulk due to the lower coordination number. Their calculated shifts indicated negative shifts on the order of 0.3 eV for iridium and platinum. Kleiman et al. [5] studied binding energy shifts by XPS for various ratios of Pt–Cu alloys and found that while Cu 2p shifted up to −0.7 eV, no shift was observed for Pt 4d lines. In regard to submonolayer thin film coverage and small clusters, both positive and negative binding energies shifts were observed relative to bulk materials. Both Mason and Baetzold [6] and Takasu et al. [4] measured positive shifts for small clusters, 2.5 eV for silver on carbon, and 1.6 eV for palladium on amorphous silver, respectively. Oberli et al. [8] measured negative binding energy shifts of 0.7 eV for the smallest gold clusters on carbon. It was concluded that none of these instances provided an explanation owing to the significant differences in material preparation and material–particle morphology. Additionally, the most significant of the binding energy shifts exceeded other reported shifts, often by more than a full order of magnitude.

The literature review also found reports of negative binding energy shifts for Group VIII metals on reduced TiO_2 catalyst supports during investigations of unusual catalytic activity attributed to strong metal support interactions (SMSI). While some of the early XPS studies of SMSI materials in the early 1980s reported negative binding energy shifts of the supported metal particles, none reported shifts below referenced metals zero valence energies. Fung [8], one of the first to report a negative binding energy shift for platinum on TiO_2 (Pt/TiO_2), reported a 1.6 eV negative binding shift for Pt4$f_{7/2}$. A closer review of the data shows that the negative shift was not below the energy of Pt^0. Instead, the negative shift was based on a comparison of binding energies obtained from vacuum deposition of platinum as a thin film (approximately one atom thick) compared to a thick film produced during typical of catalyst preparation. Chien et al. [9] reported a negative shift of 0.2 eV for Rh3$d_{5/2}$during their investigation of Rh/ TiO_2. This was also based on relative measurements between materials prepared as rhodium evaporated as a thin film on single crystals of rutile and catalyst samples prepared by impregnation. Again, the binding energies did not shift below metallic rhodium, Rh^O, the lowest valence state energy. In both instances, the negative shifts are more consistent with those observed with submonolayer coverage cited previously [5–7].

While there did not appear to be a direct correlation with SMSI investigations (the bulk of the high temperature reduction temperatures rarely exceeded 500°C since high temperatures are contra-indicated for maintaining optimal surface area for catalysis), the similarity of materials was intriguing. Information from the SMSI helped to steer a series of follow-on experiments to further elucidate the similarities in materials and differences as it related to obtaining negative binding energy shifts. Additionally, one of the proposed mechanisms to explain SMSI was based on the n-type semiconductivity (electrical conductivity) of reduced TiO_2 [4]. This was also one of the key understandings regarding the basis for the highly unusual binding energy shifts that evolved during the investigation.

This article reviews the original series of experiments designed to elucidate the cause of the unusual negative binding energy shift. We will also review and re-evaluate data from the original experiments with more recent information obtained from the literature to provide the basis for the hypothesis of the Open Gate Phenomenon. We will also show that others inadvertently overlooked data that supports the hypothesis.

2. Experimental

The materials (Rh, Pt, and Ir in TiO_2) were prepared using two different processes prior to high temperature oxidation and reduction. The initial series of materials were prepared using the Pechini process which is based on U.S. Patent 3,330,697. Materials were prepared following Example I of the patent by adding the desired amount of Group VIII metal (Rh, Pt, and Ir), from 1 to 2% mole percent ($Ti_{100-x}M_xO_2$), to prepare the resin intermediate which was calcined in air in temperatures ranging from 400 to 500°C. The subsequent material was ground with a mortar and pestle to obtain a powder which was then subjected to high temperature oxidation (100% O_2) and reduction (1% H_2 and 5% H_2in Ar) in a mullite tube furnace.

A metal salt impregnation–evaporation process was also used as a substitute for the Pechini process step prior to high temperature oxidation and reduction following the procedure for catalyst preparation outlined by Tauster et al. [12], the researchers who first identified SMSI. The materials were prepared by impregnating TiO_2 with metal salt solutions (0.5 wt.%), followed by air drying prior to high temperature oxidation and reduction. In all instances, the substituted materials were subsequently stored in plastic or glass vials under normal atmospheric conditions with no special handling precautions to maintain an inert environment prior to XPS and/or SEM/EDX analysis.

SEM analysis was performed on a JEOL JSM-35C scanning electron microscope equipped with a solid-state backscatter electron detector and Princeton Gamma-Tech X-ray detector. The samples were mounted using a conductive carbon paint/paste. A conductive carbon coating (via carbon evaporation) was not applied prior to analysis since the materials were generally sufficiently conductive to eliminate charging. SEM microprobe X-ray analysis and backscattered electron imaging using Z-contrast (imaging based on percentage of backscattered electron relative to atomic number) provided the ability to identify the location of Group VIII metals relative to TiO_2.

Two different XPS spectrometers were used for analysis. Spectrometer A was a PHI (Physical Electronics, Eden Prairie, MN) spectrometer with Auger and XPS capabilities. Spectrometer B was a Varian (Varian Analytical Instrument Devices, Palo Alto, CA) spectrometer. XPS data was typically collected within a few days of material preparation. Charge correction was based on adventitious carbon (C1s) at 284.6 eV. Except where noted, ion (Ar) sputtering was not employed prior to analysis. In order to obtain in-house reference data to compare to the PHI Handbook Data [2], XPS data was measured on pure foil and powders obtained from Alpha Products post ion sputtering.

3. Results

3.1. Initial "first incidence"

The unusual XPS data was initially observed for Rh3$d_{5/2}$ in a material (Sample 1-0) prepared with high temperature (1400°C) oxidation and reduction post-preparation of a Pechini resin intermediate to obtain a 1 mole percent rhodium substitution for TiO_2 ($Ti_{0.99}$ $Rh_{0.01}O_2$). Upon observing the initial raw data, the spectrometer was recalibrated and the sample was ion sputtered for five minutes before the second set of data was obtained and which again, confirmed the original highly unusual negative binding energy shift below the reference of 307.2 eV for Rh^0 (Table 1).

With instrument error ruled out, the issue of charge correction presented two possible options. The first used adventitious C1s for correction (284.6 eV) which resulted in lower than expected reference Ti2$p_{3/2}$energies of 458.7 eV [2]. Given the high temperature reduction, the presence of reduced species of Ti were possible which would result in a lower binding energy. Using the second option, a correction based on Ti2$p_{3/2}$,was also problematic because of the distinct possibility of reduced species. However, regardless of which charge correction was used, the magnitude of the negative shifts for Rh3$d_{5/2}$ far exceeded either charge correction option. With that in mind, electrodes (powder compressed into pellets) from the next series of materials (1600°C, and 1650°C oxidation and reduction) were analyzed by SEM prior to testing in a photo-electrochemical cell in order to determine the morphological nature of the materials.

Table 1. "First Incidence" initial data

Sample 1–0 1400°C (oxidation & reduction)	Uncorrected/corrected eV (pre-sputter)	Uncorrected/corrected eV (post-sputter)
C1*s*	286.7/284.6	284.9/284.6
Rh3$d_{5/2}$	303.3/301.2	303.0/302.7
Ti2$p_{3/2}$	458.7/456.6	NM
Ti2$p_{1/2}$	464.6/462.5	NM

NM: Not Measured

SEM examination using EDX and backscattered imaging revealed that rhodium did not appear to be substituted within the rutile structure. Instead, it was observed and detected as discrete regularly and irregularly shaped microspheres, often observed at the grain boundaries, on the surface of the TiO_2. The particles were approximately 1–10 μm in size and the irregular shape was often due to the presence of a flat surface facet interposed onto the more-or-less spherical particles. The unexpected presence of platinum with rhodium in the particles was the result of contamination from the platinum boat used to contain the material during oxidation and reduction. The temperature was sufficient for platinum to migrate and alloy with the rhodium particles. (*Note*: this practice was subsequently discontinued with future material preparations.) Subsequent XPS analysis of non-sputtered materials again confirmed substantial negative binding energy shifts for rhodium and platinum, alloyed together in the metal particles (Table 2). The data was also consistent for the presence of mixed species of titanium, Ti^{4+} and Ti^{3+}.

It is also interesting to note the presence of oxidized species of Rh^{3+} present in Sample 1–2 which was tested in a cell prior to XPS analysis in addition to a spectral line indicating a negative binding energy shift for Rh^0 (assumed species). This further confirmed the validity of the data that indicated negative binding energy shifts. It also indicated the possible presence of two different particles on the surface, those with oxidized rhodium (Rh^{3+}) and those with Rh^0 exhibiting the negative shifts. A summary of the data for the binding energy shifts of the the initial three samples is found in Table 3.

3.2. Follow-on experiments

The variables explored during the follow-on experiments were designed to understand the preparation conditions that result in negative binding energy shifts including comparable material preparation conditions to those reported for SMSI. The variables were concentrated in three areas: (1) oxidation and reduction temperature range, (2) use of a metal salt impregnation–evaporation process for the initial intermediate preparation (a replacement for the Pechini process), and

Table 2. Initial confirming data.

	Sample 1-1 1600°C (oxidation and reduction) (eV)	Sample 1-2* 1650°C (oxidation and reduction)
Rh3$d_{5/2}$	302.2	302.6 eV (Rh^0)
		308.3 ev (Rh^{3+})
Rh3$d_{3/2}$	308.6	312.7 eV (Rh^{3+})
Pt4$f_{7/2}$	62.2	NM
Pt4$f_{5/2}$	61.1	NM
Ti2$p_{3/2}$	458.0	458.0 eV
Ti2$p_{1/2}$	463.5	463.6 eV

*Post-cell testing

. References [2]: $Rh^0 - 3d_{5/2}$ is 307.2 eV and $3d_{3/2}$ is 311.9 eV.

$Pt^0 - 4f_{7/2}$ is 71.1eV and $4f_{5/2}$is 74.3 eV.

$Ti^{4+}(TiO_2) - 2p_{3/2}$ is 458.7 eV and $4f_{5/2}$is 764.4 eV.

Table 3. Summary of initial binding energy data.

Sample	Binding energy shift from Rh^0 $3d_{5/2}$ (eV)	Binding energy shift from Pt^0 $4f_{7/2}$
1-0	−6.0	NM
1-1	−5.0	−8.9
1-2	−4.6	NM

(3) substitution of other Group VIII metals, specifically platinum and iridium. Tables 4 (Pechini process preparation) and 5 (metal salt impregnation–evaporation process) provide a summary of data from the follow-on rhodium substitution experiments including varying oxidation and reduction temperatures and reduction environments ranging from 100% Ar (considered mildly reducing) to 5% H_2 in argon (the most severe).

One of the critical factors was determined to be the combination of reduction temperature and environment. Even 100% Ar at sufficiently high temperatures produced the conditions necessary for binding energy shifts. Reducing temperatures as low as 800°C were also sufficient with the more severe reduction environment (5% H_2).

The larger the microsphere, on the order of 10–20 μm and larger, the greater the propensity for irregularly shaped microspheres with angular crystal facets protruding from the relative spherical shape.

Materials were also prepared for iridium and platinum substitution (0.5 wt.%) based on the oxidation and reduction conditions required to obtain negative binding energy shifts for rhodium using the metal salt impregnation–evaporation process. Table 6 provides a summary of the experiments which resulted in negative binding energy shifts. Aside from the unusual negative shifts, consistent negative shifts without the formation of surface oxides were also observed weeks after material preparation. This was also considered highly unusual without special handling and storage of the materials.

Table 7 provides the data obtained from an experiment to illustrate the effects of high temperature oxidation and reduction on rhodium powder.

As expected, the experiment confirmed: (1) presence of surface oxides on pure rhodium metal powder without special storage, (2) high temperature exposure in air oxidizes rhodium metal powder to Rh^{3+} (Rh_2O_3), (3) high temperature

Table 4. Summary of experiments based on Pechini preparation.

No.	Substitution (mol%)	Preparation	BE shift*	Comments (XPS and SEM)
2-1	1% Rh	1650°C/O_2	2.2	Spectrometer B: Rh is oxidized which is consistent with preparation.
2-2	1% Rh	Same as 2-1 and 600°C/H_2	0.3	Spectrometer B: Rh is reduced metal with surface oxidation.
3-1	2% Rh	Same as 2-1	2.0	Same as 2-1
3-2	2% Rh	Same as 2-2	0.4	Same as 2-2
4-0	1.7% Rh	1650°C/O_2 only	1.4 and 2.0	Spectrometer B: Two distinct species of oxidized Rh. Large particles up to 20 μm in size.
4-1	1.7% Rh	Same as 4-0 and 1500°C/Ar	−1.2	Spectrometer A: Smaller regular and irregular microspheres to 1 μm at grain boundaries.
4-1			−0.6	Spectrometer B: Three weeks post preparation.
4-2	1.7% Rh	Same as 4-0 and 1400°C/Ar	−0.5	Spectrometer B:Numerous regular and irregular microspheres to 1 μm at grain boundaries.

*Pure rhodium foil reference: $Rh^0 - 3d_{5/2}$ is 307.1 eV.

Table 5. Summary of experiments based on metal salt preparation.

No.	Substitution (wt.%)	Preparation	BE shift	Comments (XPS and SEM)
5-1	0.5% Rh	800°C/O_2, 1150°C/1% H_2	−0.7	Spectrometer B Microspheres approx. 0.2 μm and less
5-1			−0.6	Spectrometer B: over a month post preparation
5-1			−1.0	Spectrometer A: two months post preparation
5-1			−0.9	Spectrometer B: four months post preparation
5-1			ND	Spectrometer B: over six months post preparation
5-2	0.5% Rh	Same as 6-1 and 800°C/1% H_2	−0.7	Spectrometer B
5-3	0.5% Rh	Same as 6-1 and 850°C/1% H_2	−0.7	Spectrometer B Microspheres are less than I μm in size
5-3			−0.6	Spectrometer B:over one month after initial testing
5-4	0.5% Rh	450°C/O_2, 850°C/1% H_2	ND	Spectrometer B: Insufficient temps for oxidation and reduction.
5-5	0.5% Rh	600°C/O_2, 800°C/1% H_2	1.2	Spectrometer B: Rhodium in oxidized state-insufficient temps for oxidation and reduction.
5-6	0.5% Rh	Salt prep and 800/O_2, 800°C/1% H_2	1.1	Spectrometer B: Rhodium in oxidized state-insufficient temps for oxidation and reduction.
5-7	0.5% Rh	1000/O_2, 800°C/5% H_2	−0.3	Spectrometer B
5-8	0.5% Rh	500°C/O_2, 800°C/5% H_2	−0.8	Spectrometer B
5-8			−0.7	Spectrometer B: six days after initial testing
5-9	0.5% Rh	500°C/O_2, 1000°C/5% H_2	−0.4	Spectrometer B

*Rh foil reference: $Rh^0 - 3d_{5/2}$ is 307.1 eV and $3d_{3/2}$ is 311.8 eV
ND- not detected.

exposure to a reducing environment removes surface oxides as does ion sputtering prior to XPS analysis, and (4) surface oxides readily form on metal powder within days of exposure to air without special storage and handling precautions. The experiment also illustrated that the high temperature oxidation and reduction required to produce negative binding energy shifts in rhodium substitute TiO_2 do not produce the same shifts in rhodium powder alone. More importantly, surface oxidation of rhodium particles does not occur when negative binding energy shifts are observed.

Overall review of the SEM and XPS data resulted in seven key observations in order to obtain negative binding energy shifts and are summarized in Table 8. It should be noted that due to the spatial resolution (area) of the XPS spectrometers, an assumption was made that the XPS data provided a representative sampling of particle sizes for the sample. This was further supported by the fact that size was generally consistent (within a relative range) for a given material preparation. Materials with small particles (in the less than 1 μm range) did not also have particles in the 10 μm and higher range.

Table 6. XPS Data for Pt and Ir substitution.

No.	Substitution	BE shift (4f 7/2)*	BE shift (4d 5/2)*	Comments
6-0	Pt	−0.3	NM	Spectrometer B
6-1	Pt	−0.7	NM	Spectrometer B
7-0	Ir	−0.7	−1.0	Spectrometer B
		−0.7	NM	Spectrometer A: 2.5 months post-preparation

*Pt foil reference: $Pt^0 - 4f_{7/2}$ is 71.1 eV.
Ir powder reference: $Ir^0 - 4f_{7/2}$ is 60.9 eV. and $4d_{5/2}$ is 297.0 eV.

Table 7. Rhodium powder surface oxidation.

No.	Preparation	Rh3d5/2 (eV)*	BE shift	Comments
A	As Received	307.5	0.4	Spectrometer B: not ion sputtered
B	900°C/air	308.5	1.4	Spectrometer B: not ion sputtered. Analyzed next day after preparation.
C	800°C/1%H_2	307.1	0.0	Spectrometer B: not sputtered. Analyzed next day after preparation
C		307.4	0.4	Analyzed (not sputtered) four days after initial analysis. No special handling or storage conditions.
C		307.1	0.0	Ion sputtered.

*$Rh^{3+} - 3d_{5/2}$ is 308.2 eV [13].

4. Discussion

4.1. Then (1982)

The three most significant observations regarding the metal particles on reduced TiO_2 (the negative binding energy shifts, the morphological shape as microspheres, and resistance to surface oxidation) indicates electron transfer from the reduced TiO_2, an n-type semiconductor, to the metal particles. This is sufficient to provide a negative charge on the particles which imparts cathodic protection from the formation of surface oxides as illustrated in Fig. 1. The transfer of electrons appeared to initiate during high temperature reduction resulting in morphological changes to the metal particles that were initially formed during high temperature oxidation. Two possible explanations for the formation of microspheres were proposed. The first was due to Gauss' law whereby the preferred shape for a point charge is a sphere to equalize charge interaction. The second derives from minimizing surface tension effects at the elevated temperatures by agglomeration.

An on-going review of the literature failed to provide any answers to explain the observations and while there appeared to be a linkage to SMSI investigations at that time due to the similarity of materials, differences in material preparation remained the critical difference, particularly in regard to the temperatures for oxidation and reduction. However, Meriaudeau et al. [10] and Chen and White [11] were some of the first to propose an electron conduction mechanism based on reduced TiO_2 as an n-type semiconductor. This supported a key understanding that evolved during the original investigation, that the fundamental mechanism for the negative binding energy shifts was associated with electron transfer from the reduced TiO_2 as n-type semiconductor to the metal particles.

The purpose of the follow-on investigation was to understand the general material preparation required to reproduce the negative binding energy shifts, and that indeed, the shifts were reproducible. No attempt was made to investigate

Table 8. Key observations.

1	Group VIII metal segregation into crystalline particles occurs during high temperature oxidation, primarily at TiO_2 grain boundaries and presumed defect sites
2	Reduction temperature and environment (in excess of 800°C) is critical to materials which exhibit binding energy shifts
3	Morphological transformation occurs from crystalline particles to microspheres during high temperature reduction of materials which exhibit binding energy shifts
4	Large microspheres on the order of 10–20 μm and larger are irregularly shaped with crystal faces protruding from the relatively spherical shape
5	Smaller binding energy shifts are observed with materials prepared with the metal salt encapsulation-evaporation process and which also produces smaller microsphere sizes
6	Binding energy shifts are observed for more than 4 months without preferential storage conditions of the materials

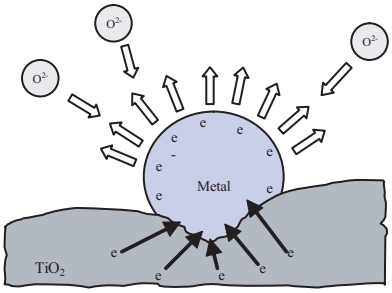

Figure 1. Cathodic protection.

any other aspect of the data, including the particle size relationship to the magnitude of the shifts and many questions remained unanswered when the investigation ended in 1982.

4.2. Now (present)

The original investigation and data was revisited more than thirty years later along with a review of the literature since that time. There is now considerably more information available concerning TiO_2 owing to its applications as a catalyst support, and in particular, as a photocatalyst. With one exception, the literature still does not show any instances of similar experimentation and data. However, a review of the literature provides information which further contributes to an understanding of the original investigation.

One area of interest is specifically related to the anatase-rutile transformation temperature for TiO_2. The threshold temperature of approximately 800°C was determined to be the lower threshold to produce the negative shifts which was lower than the presumed (in 1982) threshold of approximately 1000°C for the anatase-rutile transformation. A more recent paper by Gouma et al. [14] studying anatase-rutile transformation referenced research dating back 50 years to a paper by Shannon and Pask [15] with data that indicated that the transformation can occur as low as 400°C depending upon the synthesis method, the atmosphere, and the presence of other ions. They noted that reduction increases the rate and lowers the transformation temperature due to oxygen vacancies. This confirmed a study by Iida and Ozaki [16], where rutile transformation was enhanced by a reducing environment (argon, hydrogen, and vacuum). Their studies also found that additions of transition metals can promote the transformation at lower temperatures. Therefore, although the specific causal link is not currently understood, the threshold temperature required to obtain negative shifts is linked to the transformation to the rutile TiO_2.

Based on this information, a clearer understanding evolved for the conditions required to prepare materials which exhibit negative binding energy shifts: (1) material preparation that contributes to intimate mixing of metal oxides with TiO_2 and subsequent mobility that accompanies high temperature oxidation, (2) sufficient reduction of TiO_2 to an n-type semiconductor, and (3) transformation of TiO_2 to the rutile structure. The high temperature oxidation allows the metal to grow from the TiO_2 substrate (regardless of the initial pre-oxidation preparation) as opposed to a deposition onto a TiO_2 support. This implies an inherent difference between a metal-substrate interface as opposed to a metal-support interface. Herein is a key to understanding the basis for the mechanism that results in negative shifts. With this in mind, a review of SMSI-related literature also provides information which further supports the original investigation.

SMSI-related research exploded in the mid-1980s beyond the original catalysis investigations. This included experiments designed to test for electron transfer of metals deposited onto single crystal TiO_2 using surface analysis techniques as well as investigations into other reducible oxides and the use of dopants to explore the semi-conductor properties of reduced TiO_2. Unfortunately, no single electronic-based hypothesis could explain the often mixed and

confusing results with the widely ranging materials preparations from real-catalyst to single crystal in-situ preparations. An alternative explanation evolved based on data that indicated encapsulation of the metal particles by a TiO suboxide layer which, with a few exceptions, is currently the preferred explanation for SMSI. However, a few more recent catalysis studies, including gold on reduced TiO_2, also continue to provide additional support to the original SMSI investigations of real catalysts where an electronic basis was first postulated.

In a study of real Au/TiO_2 catalysts (prepared using a metal salt impregnation–evaporation process, not single crystal in-situ preparations) in 2001, Akita et al. [17] found preferential nucleation of gold clusters on rutile structures prepared at different calcination temperatures. Their data indicated preferential nucleation of Au particles at grain boundary interfaces and that it initiates during calcination (high temperature oxidation). They also noted a "significant difference between catalyst prepared by deposition precipitation [polycrystalline] and a model catalyst made by evaporation of gold onto the surface of a single crystal of rutile."

In 2003, Eider and Kramer [18] investigated the structural and electronic effects of high reduction temperatures of real Pt/TiO_2 catalysts. The reduction temperatures for this study ranged up to 800°C, higher than many previous studies and which is a temperature sufficient for complete transformation to rutile. Their findings were significant in regard to the affects of temperature on grain size, surface area, and conductivity. They concluded that the "higher density of charge carriers causes a narrowing of the space charge region at the metal support phase boundary" and that the "charge transfer necessary to align the Fermi levels of the two phases becomes larger which most likely affects the catalytic properties of these catalysts."

In 2005 paper, Iddir et al. [19], also studying real Pt/TiO_2 catalysts observed an "unexpected" preferential nucleation for Pt particles on rutile over anatase with reduction and that the distribution of Pt seemed independent of surface orientation of TiO_2 particle with a higher concentration at the TiO_2 particle edges. They also observed a "nearly perfect spherical shape and thus has a point-like contact with titania [TiO_2]" which as they explained "shows the complex inter-dependence between the Pt particle shape, Pt–TiO_2 interface extent, TiO_2 phase, surface crystallographic orientation, and possibly the local density of oxygen vacancies." Although their investigation did not include any XPS analysis, their results support the effects of charge transfer on the morphology of the supported metal particles. Micrographs using Z-contrast (backscattered electron imaging) are particularly reminiscent of observations in the original investigation.

All of these papers concur with the findings of this paper and reinforces the complexity of polycrystalline TiO_2. However, a paper published in 1986 provided data that directly supported the original negative shift investigations. Spichiger-Ulmann et al. [20] prepared Pt/TiO_2 catalyst materials for XPS analysis using salt impregnation-evaporation of thick films (10–15 μm) of TiO_2 followed by air calcination and reduction in argon. Subsequent XPS analysis reported negative binding energy shifts from 0.2 to 0.6 eV for Pt particles (less than 1 μm) below their Pt^0 reference (prepared as a thick film on titanium). Additionally, the negative binding energy shifts were "persistent even after exposure of the samples to air for several days" and in one sample, up to four months before a positive shift back to a binding energy relative to the standard. Their findings correlate well with the original investigations presented in this paper and are also expected given their material preparation and calcination (oxidation) and reduction temperatures (up to 550°C).

They recognized the earlier work of Meriaudeau et al. and Chen and White in regard to the shifts explained in terms of Fermi energy adjustment between the reduced TiO_2 and metal resulting in the formation of a Schottky barrier. However, they considered this assumption problematic owing to the size of the particles on the surface and the assumption, in principle, of a region of less than 0.5 nm in which a significant change of electron density would be expected. The size of the particles were too large relative to the assumed size and nature of the space charge layer of the barrier. They concluded that encapsulation could just as easily be an explanation.

It is important to consider the general assumptions of the time in order to understand the context of their assumptions. This paper was first presented in 1985 at a symposium sponsored by the American Chemical Society during the height of investigations into an electronic hypothesis but also during the earliest hypotheses of encapsulation. Additionally, the assumptions about Schottky barriers was (and is) based on a metal deposited onto a semiconductor, not grown from

the semiconductor itself. Understanding this difference is one of the key elements to understanding the cause of the negative shifts, and more importantly, the cause and underlying mechanism.

4.3. Open gate hypothesis

In metal–semiconductor contact theory, thermodynamic equilibrium assumes that the electrochemical potential is uniform throughout the system. A potential forms at the junction of a metal and semiconductor, a Schottky barrier, based on their respective differences in electrochemical potentials. The ideal barrier height is determined by

$$\phi_B = \phi_M - \chi_S,$$

where ϕ_M is the work function of the metal and χ_S is the electron affinity of the semiconductor. As contact is made, electrons will flow initially to the material with the smaller potential. However, as the barrier forms, the flow of electron slows and eventually stops due to the formation of a depletion (of charge) zone, the charge neutral layer (CNL). In traditional semiconductor fabrication and applications, the presence of a thin layer of interfacial oxides is also a significant factor determining the actual barrier height.

Additional factors are taken into consideration with metal–semiconductor contacts in regard to Group VIII metals. For Rh, Ir, and Pt in contact with TiO_2, the contact potential is the difference in work functions: 4.6 eV [21] for reduced TiO_2, 4.98 eV for Rh, 5.61 eV for Ir (average for 100, 110, and 111 crystal planes) and 5.64 eV for Pt [22]. This results in electrons transferred to the metal particles. For TiO_2 which is a strongly ionic semiconductor, the Schottky barrier height will be equal or proportional to the difference in work functions. In regard to the amount of charge transferred, it is assumed to be significant since TiO_2 has a very high static dielectric constant and that there will be a strong dipole at the metal–TiO_2 interface. It is also assumed that while the affected volume of charge depletion in TiO_2 will be substantially larger (on the order of 10^6), the charge in the metal will remain at the interface due to the effective screening of metal electrons ([23] and references therein). In the case of small metal particles, the electric field will be dependent upon the metal–particle diameter. Nevertheless, the charge at the free metal surface will be negligible. Herein is the apparent departure from traditional metal–semiconductor assumptions for the Open Gate hypothesis.

Three elements are key to understanding the underlying mechanism of the negative shifts. The first is that although Group VIII metals on reduced TiO_2 are Schottky metals on an n-type semiconductor, the metal–semiconductor interface is not the same in the traditional sense of a fabricated Schottky diode. The metal particles coalesce from the TiO_2 substrate thereby providing a very different interface than metallization applied to a semiconductor support during diode fabrication.

The second element is that the negative shifts occur in polycrystalline materials. Polycrystalline materials have grain boundaries and defect sites which affect electrical properties relative to a single crystal. While no metal was detected within the rutile lattice, this was not confirmed using another more precise analytical technique and therefore some level of metal doping of the rutile lattice may also contribute to the mechanism. Taken altogether, this adds to the complexity of understanding electron transport and conductivity of reduced TiO_2.

However, what is the consistent with metal–semiconductor theory is that the junction is rectifying. The electrons flow one-way from the n-type semiconductor into the Schottky metal. This is the third element and critical piece in understanding the cause of the negative shifts. The shifts are caused by an isolated (one-way) negative charge on the metal particles. This is best understood by understanding what affects binding energies and how binding energies are measured in an XPS spectrometer.

The binding energy of an electron depends on the energy level from which it originates ($1s$, $2s$, $2p_{3/2}$, etc. …) but also on the oxidation state of the atom as well as the local chemical and physical environment. The binding energies derived from measurements in a spectrometer are based on the following:

$$E_{binding} = E_{photon} - E_{kinetic} - \phi,$$

E_{photon} is the energy of the excitation radiation and ϕ is the work function of the spectrometer (not the material/sample analyzed). The key assumption is that both the sample and the spectrometer are at the same potential (grounded to one another). However, if an external voltage is applied to a sample which was isolated (not at ground with the spectrometer), then the binding energies of the isolated sample shift relative to the applied voltage. Herein is the explanation for the negative binding energy shifts. The metal particles are isolated from the TiO_2 substrate and therefore from the spectrometer due the rectifying interface between reduced TiO_2 and the metal particles. The negative binding shifts are the result of the local environment alone created by the transfer of electrons from reduced TiO_2 (n-type semiconductor) and the metal particles (Schottky metal). The negative charge on the particles **is** the local environment and explains why corresponding shifts were not observed for titanium binding energies.

It would initially appear that the observations for negative shifts observed in the iridium substitution material (Sample 7-0) are not consistent because of the difference in the magnitude of the binding energy shifts for the energies for Ir4$f_{7/2}$ and Ir4$d_{5/2}$ (0.7 eV versus 1.0 eV). This difference, however, may be attributed to the differences in the shielding effects related too the relative radius differences of the electron orbitals [24]. This may also be a factor in the difference in shifts observed in Sample 1-1 between Rh3$d_{5/2}$and Pt4$f_{7/2}$where the metals are alloyed in the same microspheres.

However, the electron flow and resultant negative charge on the metal particles is also not the result of X-ray photon excitation during the XPS examination. The flow of electrons from TiO_2 into the metal is established during high temperature reduction and is of sufficient magnitude to affect morphological changes in the particles exhibiting the negative charge. Due to Gauss' law, the preferred shape is a sphere for a point charge to equalize charge interaction. The metal microspheres are therefore a conducting sphere where the charge resides on the surface, instead of only at the interface. However, at a given magnitude of charge on a microsphere relative to its size (radius), the energy balance tips in favor of the crystal lattice structure. This explains the observations of crystal facets and edges protruding from some of the very large microspheres. While this implies a limiting factor as to the size of the charge on the particles-microspheres, the charge is also of sufficient durability to provide cathodic protection from surface oxidation of the metal particles over an extended period of time.

In the material (Sample 5-1) where the negative shift was observed at 4.5 months, no rhodium was detected after 6 months (Table 5). This along with other anomalous data suggested a carbon-based surface contamination on the sample, perhaps plasticizer from the plastic vial. Unfortunately, this was at the end of the investigation and no further experimentation was performed to resolve the inconclusive results. However, in the Spichiger–Ulmann study, a positive shift relative to the reference value for $Pt^0$was observed in the sample after four months of air exposure indicate. This is understood to indicate a loss of the negative charge on the metal particles.

It is therefore proposed that the underlying mechanism for the Open Gate Phenomenon is based on a unique metal–semiconductor interface that results from metal particles grown from the semiconductor itself. The interface significantly affects the Schottky barrier height and CNL resulting in a one-way open gate for electron flow from the reduced TiO_2 to the metal particles based on their difference in work function. The result is a significant and durable negative charge (electron transfer) to the metal particles.

Any conjecture beyond this basic hypothesis is difficult. Many questions remain unanswered. Assuming that there are factors which limit the negative charge on the metal particles, is it based on metal particle size or, something associated with the reduced TiO_2 itself? Is there a charge–discharge cycle associated with it? Is the loss of cathodic protection from surface oxidation attributed to the loss of conductivity of the TiO_2 with its re-oxidation during air exposure, or is there another mechanism involved?

Of course, the most important unanswered question revolves around what initiates and maintains the charge. Is it possible that the electron flow into the metal particles is as simple as that work function equilibrium is not attained? Why not? Is the source of electrons only those contained within the materials? Depending upon the answers to these questions, the Open Gate Phenomenon has the potential to become the foundation of a new energy technology.

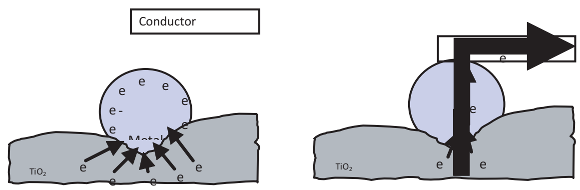

Figure 2. Current (electron flow) to a conductor.

From an application standpoint for a new energy technology, the behavior of metal microspheres may be comparable to miniaturized Van de Graff generators. Borrowing on the concept that Van de Graff generators are a nearly ideal current source derived from an electrostatic generator, the metal microspheres may also provide for direct electrical energy generation. Figures 2 and 3 illustrate this concept based on a series of connected parallel plates on which a thick-film of an Open Gate Phenomenon-based metal oxide is prepared with a metal (ground support) and conductive over-layer providing a connection to the negatively charged microspheres. However, unlike with an electrochemical-based battery, connecting to ground (a source of free electrons) does not short-out the device because of the inherent one-way gate (diode) of the interface. The black box is an internal circuit that may be required if the mechanism has a charge–discharge cycle associated with it.

5. Conclusions

The Open Gate hypothesis is based on readily observable and reproducible experimental results. Additional in-depth research is required to investigate the full nature of the interface and mechanism that results in the unusual negative charge on Group VIII metal particles grown from reduced rutile TiO_2. Once this is more fully understood, the Open Gate Phenomenon may be applicable to other appropriate metal–reducible oxides and mixed metal oxides. Based on the preliminary findings, the Open Gate Phenomenon has the potential to become the foundation for a new technology with direct and indirect energy applications including catalysts and electrocatalysts, particularly for fuel cells.

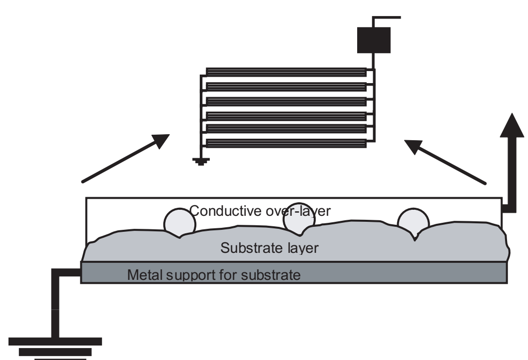

Figure 3. Concept of a device for direct electrical energy generation.

References

[1] U.S. Patent 3,330,697; Maggio Pechini, inventor; Method of Preparing Lead and Alkaline Earth Titanates and Niobates and Coating Method using the Same to Form a Capacitor. July 11, 1967.

[2] *Handbook of X-Ray Photoelectron Spectroscopy*, Perkin Elmer Corporation, Physical Electronics Division, Eden Prairie, MN, USA, 1979.

[3] B. Johansson and N. Martensson, Core-level binding energy shifts for the metallic elements, *Phys. Rev.* B **21** (1980) 4427.

[4] G.G. Kleiman, V.S. Sundaram, C.L. Barreto and J.D. Rogers, ESCA determination of the electronic structure of Pt–Cu alloys, *Solid State Communications* **32** (1979) 919.

[5] M.G. Mason and R.C. Baetzold, ESCA and molecular orbital studies of small silver particles, *J. Chem. Phys.* **64** (1976) 271.

[6] Y. Takasu, B. Unwin, B. Tesche and A.M. Bradshaw, Photoemission from palladium partical arrays on an amorphous silica substrate, *Surface Sci.* **77** (1978) 219.

[7] L. Oberli, R. Monot, H.J. Mathieu, D. Landolt and J. Buttet, Auger and X-ray photoelectron spectroscopy of small Au particles, *Surface Sci.* **106** (1982) 301.

[8] S.C. Fung, XPS studies of strong metal-support interactions (SMSI)–Pt/TiO_2, *J. Catal.* **76** (1982) 225.

[9] S.H. Chien B.N. Shelimov, D.E. Resasco, E.H. Lee and G.L. Haller, Characterization of the interaction between Rhodium and titanium oxide by XPS, *J. Catal.* **77** (1982) 301.

[10] O. Meriaudeau, O.H. Ellestad, M. Dufaux and C. Naccache, Metal–support interaction: catalytic properties of TiO_2–supported platinum, iridium, and rhodium, *J. Catal.* **75** (1982) 243.

[11] B.H. Chen and J.M. White, Properties of platinum supported on oxides of titanium, *J. Phys. Chem.* **86** (1982) 3534.

[12] S.J. Tauster, S.C. Fung and R.L. Garten, Strong metal support interactions, group 8 nobel metals supported on TiO_2, *J. Catal.* **100** (1978) 170.

[13] Y. Okamato, N. Ishida, T. Imanaka and S. Teranishi, Active states of rhodium in rhodium exchanged Y zeolite catalysts, *J. Catal.* **58** (1979) 82.

[14] P.I. Gouma, M.J. Mills and G.S. Rohrer, Anatase-To-rutile transformation in titania powders, *J. Am. Ceramic Soc.* **284** (2001) 619.

[15] R.D. Shannon and J.A. Pask, Kinetics of the anatase-rutile transformation, *J. Am. Ceramic Soc.* **48** (1965) 391.

[16] Y. Iida and S. Ozaki, Grain growth and phase transformation of titanium oxide during calcination, *J. Am. Ceramic Soc.* **44** (1961) 120.

[17] T. Akita, L. Ping, S. Ichikawa, K. Tanaka and M. Haruta, Analytical TEM study on the dispersion of Au nanoparticles in Au/TiO_2 catalyst prepared under various temperatures, *Surf. Interface Anal.* **31** (2001) 73.

[18] D. Eder and R. Kramer, Stoichiometry of "Titanium Suboxide": Part 2. Electric properties, *Phys. Chem. Chemeical Phys.* **5** (2003) 1314.

[19] H. Iddir, M.M. Disko, S. Ogut and N.D. Browning, Atomic scale characterization of the Pt/TiO_2 interface, *Micron* **36** (2005) 233.

[20] M. Spichiger-Ulmann, A. Monnier, M. Koudelka and J. Augustynski, *Spectroscopic and Electrochemical Study of the Sate of* Pt *in* Pt–TiO_2 *Catalysts*, *Strong Metal Support Interactions*, R.T.K. Baker, S.J. Tauster and J.A. Dumesic (Eds.), American Chemical Society Washington, DC, 1986, p. 212.

[21] Y.W. Chung, W.J. Lo and G.A. Somorjai, Low energy electron diffraction and electron spectroscopy studies of the clean (110) and (100) titanium dioxide (rutile) crystal surfaces, *Surface Sci.* **64** (1977) 588.

[22] *CRC Handbook of Chemistry and Physics*, David R. Linde (Editor-in-Chief), CRC Press, Boca Raton, FL, 2008, pp. 12–119.

[23] X.E. Verykios, Support Effects on Catalytic Performance of Nanoparticles. Catalysis and Electrocatalysis at Nanoparticle Surfaces, A. Wieckowski, E.E. Savinova and C.G. Vayenas (Eds.), Marcel Dekker, New York, 2003, p. 745, and references herein.

[24] Carlson Thomas A., *Photoelectron and Auger Spectroscopy*, Plenum Press, New York, 1975.